Direct Structural Annotation of Membrane Protein Aggregation Loci using Peptide–Based Reverse–Mapping

Muralikrishna Lella[1] *and Radhakrishnan Mahalakshmi*[1*]

[1]Molecular Biophysics Laboratory, Department of Biological Sciences, Indian Institute of Science Education and Research Bhopal, Bhopal – 462066. India.

*E-mail: maha@iiserb.ac.in

SUPPORTING INFORMATION

MATERIALS AND EXPERIMENTAL METHODS

Reagents and chemicals

We purchased Rink Amide AM resin (200-400 mesh, 0.63 mmol/g loading capacity) from Novabiochem® (Merck Life Science Pvt. Ltd.). N,N-Dimethylformamide (DMF), N,N-diisopropylethylamine (DIPEA), trifluoroacetic acid (TFA), triisopropylsilane (TIPS), thioanizole, thioflavin (ThT) and Kaiser test reagents were purchased from Sigma-Aldrich Co. LLC. We obtained all N^{α}-Fmoc protected amino acids with > 98% purity, and 2-(1H-7-azabenzotriazol-1-yl)-1,1,3,3-tetramethyl uranium hexafluorophosphate methanaminium (HATU) from GL Biochem Shanghai Ltd. 1-hydroxybenzotriazole hydrate (HOBt) was purchased from Spectrachem Pvt. Ltd. Unless otherwise specified, all reagents and chemicals were of >99% purity and were used without further purification or processing.

Peptide synthesis, purification, and mass spectrometric analysis

Peptide synthesis was carried out on Rink Amide AM resin in dry DMF using Fmoc-protected amino acids. Combined activation and coupling of amino acids was achieved using HOBt/ HATU/ DIPEA. 20% piperidine in DMF was used to remove the Fmoc protecting group. The complete synthesis was carried out at 37 °C and monitored at each step by using the Kaiser test. After completion of the synthesis, the peptide was simultaneously cleaved from the resin and the side chains were deprotected by incubating at 25 °C for 8–10 h, in a cleavage cocktail containing TFA (88% v/v), phenol (5% v/v), water (5% v/v), and TIPS (2% v/v). The cleavage solution was filtered and evaporated under vacuum using a rotatory evaporator. The peptide washed 3–4 times with cold diethyl ether by high-speed centrifugation. The precipitated peptide was lyophilized to obtain the peptide as a powder. Purity of the peptide was checked using analytical high performance liquid chromatography (HPLC) on a C_{18} column (5 μm particle size) by elution using a H_2O: CH_3OH binary gradient from 20 to 85 % CH_3OH for 35 min. The mass spectra of all the peptides were recorded immediately after synthesis on an Esquire 3000 plus ion trap mass spectrometer (Tables S1-S4 and Figures S1-S3).

Sample preparation for peptide aggregation studies

We tried several methods to dissolve the peptide into the buffer medium. We identified difficulties with most of the methods, due to the highly hydrophobic nature of the hVDAC peptides. We were able to attain identical starting concentrations for the all peptides only using one protocol, wherein we employed a TFA mediated transfer process to the desired buffer conditions. Here, all the peptides were prepared by dissolving in neat TFA to achieve a stock peptide concentration of 20 mM. The peptide stock was diluted to achieve final concentrations of 0.2 mM, 0.4 mM and 0.5 mM in 50 mM sodium citrate buffer pH 4.0 (SCB) or 50 mM sodium

phosphate buffer pH 7.2 (SPB). The acidity of TFA was neutralized by adding the required volume of 10 N sodium hydroxide in both buffer conditions. Additionally, 0.02% (3 mM) sodium azide was used in all the buffers to suppress bacterial or fungal growth during the 30-day incubation period. We ensured that TFA, NaOH and sodium azide did not interfere in our measurements by checking with the proper controls. To observe the aggregation propensity of the peptide, 12.5 μM of ThT was added to the sample. The final volume of each sample after addition of all the reagents was 200 μl. The buffer blanks were prepared as mentioned above but without peptide addition.

ThT fluorescence measurements of peptide aggregation

ThT fluorescence was measured on a multimode microplate reader (SpectraMax M5, Molecular Devices, LLC). Peptide samples, prepared as outlined above, were incubated in a humidity controlled chamber at 25 °C. The progress of aggregation was monitored every 12 h for 30 days at 25 °C. Here, ThT in the peptide samples was excited at a λ_{ex} = 445 nm and the emission spectra were recorded from 465 nm to 530 nm, with an excitation cut-off of 475 nm. The emission maximum of ThT fluorescence was observed at 485 nm and the fluorescence intensity at this wavelength was plotted as a function of time, to observe the peptide aggregation kinetics. All the data were averaged over a minimum of three independent sample preparations in each condition. In specific samples where high peptide aggregation propensity was observed, the data at 465 nm was also plotted and processed.

SEM imaging of peptide aggregates

Scanning electron microscopy (SEM) was performed to identify the morphology of the aggregated peptides. Only those samples containing a peptide concentration of 0.5 mM in SCB were used for imaging. Samples in SPB showed considerable interference from the buffer, and were not processed for SEM. The aggregated samples were diluted considerably for SEM experiments, to observe well-separated images of the peptide aggregates. Samples for imaging were prepared as follows. A 10 μl of the aggregated sample was diluted in 10 μl of SCB. This sample was spotted on aluminum SEM stubs with double-sided carbon tape; samples were air dried at 30 °C for 16–18 h. The dried samples were gold coated using a Q150R ES rotary-pumped sputter coater instrument from Quorum Technology. The coating was done for 120 s. The gold-coated peptide aggregates were imaged using the Zeiss UltraPlus FE-SEM high-resolution field emission scanning electron microscope. An accelerating voltage of 10 kV was used.

Differential interference contrast (DIC) and fluorescence microscopy

The samples that contained 0.5 mM peptide were used for imaging. The sample preparation was as follows. A 5–10 μl aliquot of aggregated peptide was spotted on a glass slide

and mounted with a cover slip. Bright field DIC, GFP and DAPI filters were used to acquire the fluorescence images of ThT bound peptides. The images were acquired by using 65X and 100X objective lenses with oil emulsion, on a Leica DM 2500 with high-end CCD Camera DFC365 FX (Leica Microsystems CMS GmBH). The same image processing was applied to all the peptide samples.

Peptide ThT fluorescence data fitting on AmyloFit

The ThT fluorescence data (λ_{em} at 485 nm) was used to understand the molecular mechanism of peptide aggregation and the half-time of peptide aggregation was derived. The fitting was carried out using the AmyloFit tool.[1] The default parameters available with the software were followed. Briefly, the ThT fluorescence intensity at each concentration was normalized between 0 and 1 by using pre- and post-transition data points as baselines. We obtained the best fit of our data to the equation describing a secondary nucleation dominated mechanism for aggregation.[2] We maintained 40–50 basin hoops for the improvement of fitting. After completion data fitting, half-times ($t_{1/2}$) were calculated using the instructions provided in AmyloFit.[1]

SUPPLEMENTARY TABLES

Table S1. List of hV1 peptide sequences described in this study with their calculated and observed molecular weights.

Strand name	Sequence	No. of residues	M_{calc} (Da)	M_{obs} (Da)[@]
α1	**MAVPPTYADLGKSARDVFTKG**	21	2222.14	1112.4 ($2H^+$)
β1	**LIKLDLKTK**	09	1069.71	1070.6 (H^+)
β2	**LEFTSSGSA**	09	896.41	897.2 (H^+)
β3	**KVTGSLETKYRW**	12	1465.79	1466.7 (H^+)
β4[#]	**LTFTEKW**	07	922.48	923.4 (H^+)
β5	**NTLGTEITVE**	10	1074.54	1075.4 (H^+)
β6	**LKLTFDSSF**	09	1055.55	1056.4 (H^+)
β7	**GKKNAKIKTGYK**	12	1333.81	1334.7 (H^+)
β8	**INLGSDMDF**	09	1009.44	1010.3 (H^+)
β9	**GPSIRGALVLGY**	12	1200.68	1201.6 (H^+)
β10	**WLAGYQMNF**	09	1127.51	1128.4 (H^+)
β11	**RVTQSNFAVGYK**	12	1367.72	1368.5 (H^+)
β12[#]	**FQLHTNVN**	08	970.48	971.4 (H^+)
β13[#]	**TEFGGSIYQK**	10	1127.55	1128.4 (H^+)
β14	**LETAVNLAWT**	10	1115.58	1116.5 (H^+)
β15	**RFGIAAKYQID**	11	1279.69	1280.5 (H^+)
β16	**ASFSAKV**	07	707.39	708.2 (H^+)
β17[#]	**SLIGLGYTQTL**	11	1163.64	1164.5 (H^+)
β18	**IKLTLSALLD**	10	1084.67	1085.6 (H^+)
β19	**KLGLGLEFQ**	09	1002.57	1003.5 (H^+)

[#]These peptide sequences are identical in hV1 and hV2 or hV1 and hV3; in these cases, data obtained from the same peptide is used for all three proteins, where appropriate.
[@]Ionization state and species observed on the ESI-MS is provided in brackets.

Table S2. List of hV2 peptide sequences described in this study with their calculated and observed molecular weights.

Strand name	Sequence	No. of residues	M_{calc} (Da)	M_{obs} (Da)[@]
α1	**AIPPSYADLGKAARDIFNKG**	20	2102.11	1052.3 ($2H^+$)
β1	**LVKLDVKTK**	09	1041.68	1042.7 (H^+)
β2	**VEFSTSGSS**	09	898.39	899.3 (H^+)
β3	**KVTGTLETKYKW**	12	1451.80	1452.7 (H^+)
β4[#]	**LTFTEKW**	07	922.48	923.4 (H^+)
β5	**NTLGTEIAIE**	10	1058.55	1081.4 (Na^+)
β6	**LKLTFDTTF**	09	1083.58	1084.5 (H^+)
β7	**GKKSGKIKSSYK**	12	1308.77	1309.7 (H^+)
β8	**INLGSDVDF**	09	977.47	978.3 (H^+)
β9	**GPAIHGSAVFGY**	12	1173.58	1174.5 (H^+)
β10	**WLAGYQMTF**	09	1114.51	1115.4 (H^+)
β11	**KLTRNNFAVGYR**	12	1436.79	719.2 ($2H^+$)
β12[#]	**FQLHTNVN**	08	970.48	971.4 (H^+)
β13[#]	**TEFGGSIYQK**	10	1127.55	1128.4 (H^+)
β14	**LDTSVNLAWT**	10	1117.56	1118.5 (H^+)
β15	**RFGIAAKYQLD**	11	1279.69	1280.6 (Na^+)
β16	**ASISAKV**	07	673.40	674.1 (H^+)
β17	**SLIGVGYTQTL**	11	1149.63	1150.6 (H^+)
β18	**VKLTLSALVD**	10	1056.64	1057.6 (H^+)
β19	**KVGLALELE**	09	969.57	970.5 (H^+)

[#]These peptide sequences are identical in hV2 and hV1 or hV2 and hV3; in these cases, data obtained from the same peptide is used for all three proteins, where appropriate.
[@]Ionization state and species observed on the ESI-MS is provided in brackets.

Table S3. List of hV3 peptide sequences described in this study with their calculated and observed molecular weights.

Strand name	Sequence	No. of residues	M_{calc} (Da)	M_{obs} (Da)[@]
α1	**MSNTPTYSDLGKAAKDVFNKG**	21	2242.09	1122.3 ($2H^+$)
β1	**MVKIDLKTK**	09	1073.65	1074.5 (H^+)
β2	**VEFSTSGHA**	09	932.42	933.3 (H^+)
β3	**KASGNLETKYKV**	12	1335.74	668.7 ($2H^+$)
β4	**LTFTQKW**	07	921.49	922.3 (H^+)
β5	**NTLGTEISWE**	10	1147.54	1148.4 (H^+)
β6	**LKLTLDTIF**	09	1061.64	1062.5 (H^+)
β7*	**KSGKLKASYK**	10	1107.66	1108.5 (H^+)
β8	**FSVGSNVDI**	09	935.46	936.3 (H^+)
β9	**GPTIYGWAVLAF**	12	1292.68	1293.6 (H^+)
β10	**WLAGYQMSF**	09	1100.50	1101.4 (H^+)
β11	**KLSQNNFALGYK**	12	1380.74	691.2 ($2H^+$)
β12	**FQLHTHVN**	08	993.50	994.4 (H^+)
β13[#]	**TEFGGSIYQK**	10	1127.55	1128.4 (H+)
β14	**IETSINLAWT**	10	1145.59	1146.5 (H^+)
β15	**RFGIAAKYMLD**	11	1282.67	1283.5 (H^+)
β16	**TSLSAKV**	07	703.41	704.2 (H^+)
β17[#]	**SLIGLGYTQTL**	11	1163.64	1164.5 (H^+)
β18	**VKLTLSALID**	10	1070.66	1071.6 (H^+)
β19	**KVGLGFELE**	09	989.54	990.5 (H^+)

[#]These peptide sequences are identical in hV3 and hV1 or hV3 and hV2; in these cases, data obtained from the same peptide is used for all three proteins, where appropriate.
[@]Ionization state and species observed on the ESI-MS is provided in brackets.
*hV3-β7 peptide does not contain the first two N-terminal amino acids (GK).

Table S4. List of hybrid peptide sequences described in this study with their calculated and observed molecular weights.

Strand name	**Sequence**	**No. of residues**	**M_{calc} (Da)**	**M_{obs} (Da)[@]**
β11a	**KLTQNNFAVGYR**	12	1408.74	1409.7 (H^+)
β11b	**KLTRNNFAVGYK**	12	1408.78	1409.8 (H^+)

[@]Ionization state and species observed on the ESI-MS is provided in brackets.

SUPPLEMENTARY FIGURES

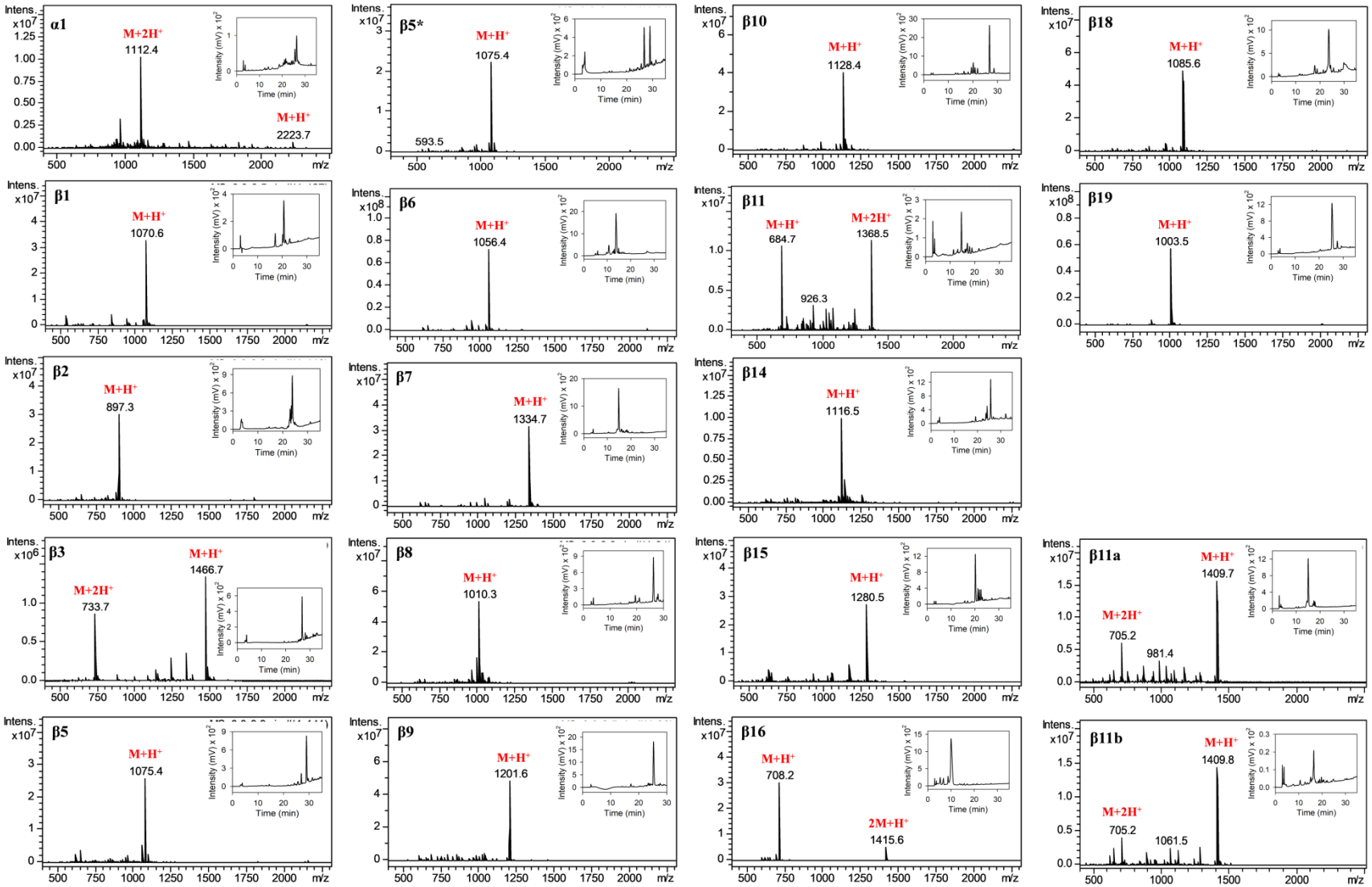

Figure S1. Mass spectra and analytical RP-HPLC profiles of hV1 peptides and hybrid peptides of hV-β11. Each graph shows the ESI-MS spectrum highlighting the H^+ and $2H^+$ adducts of the peptide (peptide name provided within each panel). Inset shows the analytical RP-HPLC profile of the crude peptide analyzed using a water-methanol gradient. The hV1-β5 showed inconsistent aggregation in our experiments. Here, β5* denotes the HPLC profile recorded after one month of peptide preparation, where we observe two major peaks corresponding to the expected peptide molecular weight. We suspect that a non-proline mediated *cis-trans* isomerization exhibited by the peptide may give rise to the observed peaks with different retention times on RP-HPLC. The exact origin of this anomaly is unclear, and is being investigated further.

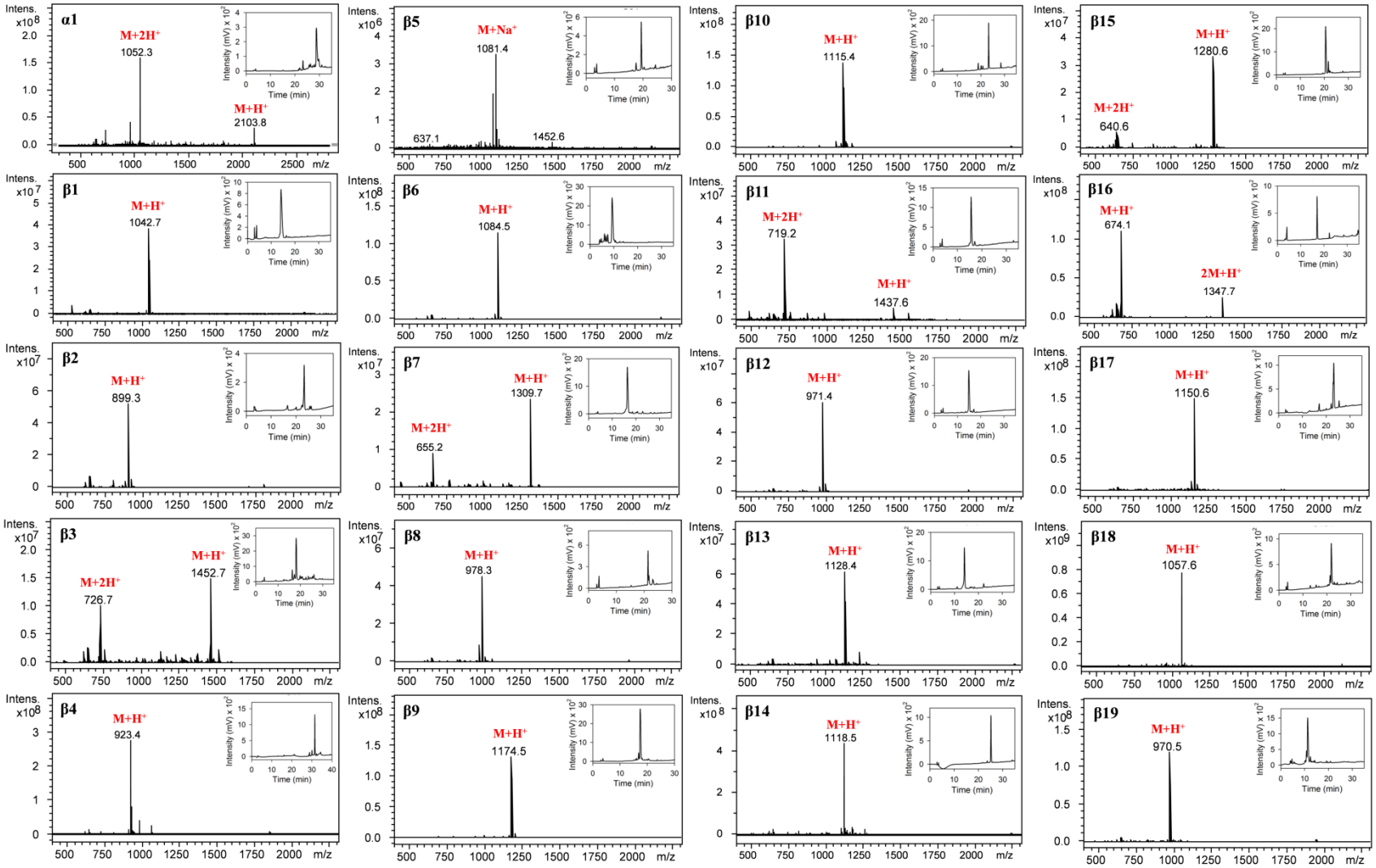

Figure S2. Mass spectra and analytical RP-HPLC profiles of hV2 peptides. Each graph shows the ESI-MS spectrum highlighting the H^+ and $2H^+$ adducts of the peptide (peptide name provided within each panel). Inset shows the analytical RP-HPLC profile of the crude peptide analyzed using a water-methanol gradient.

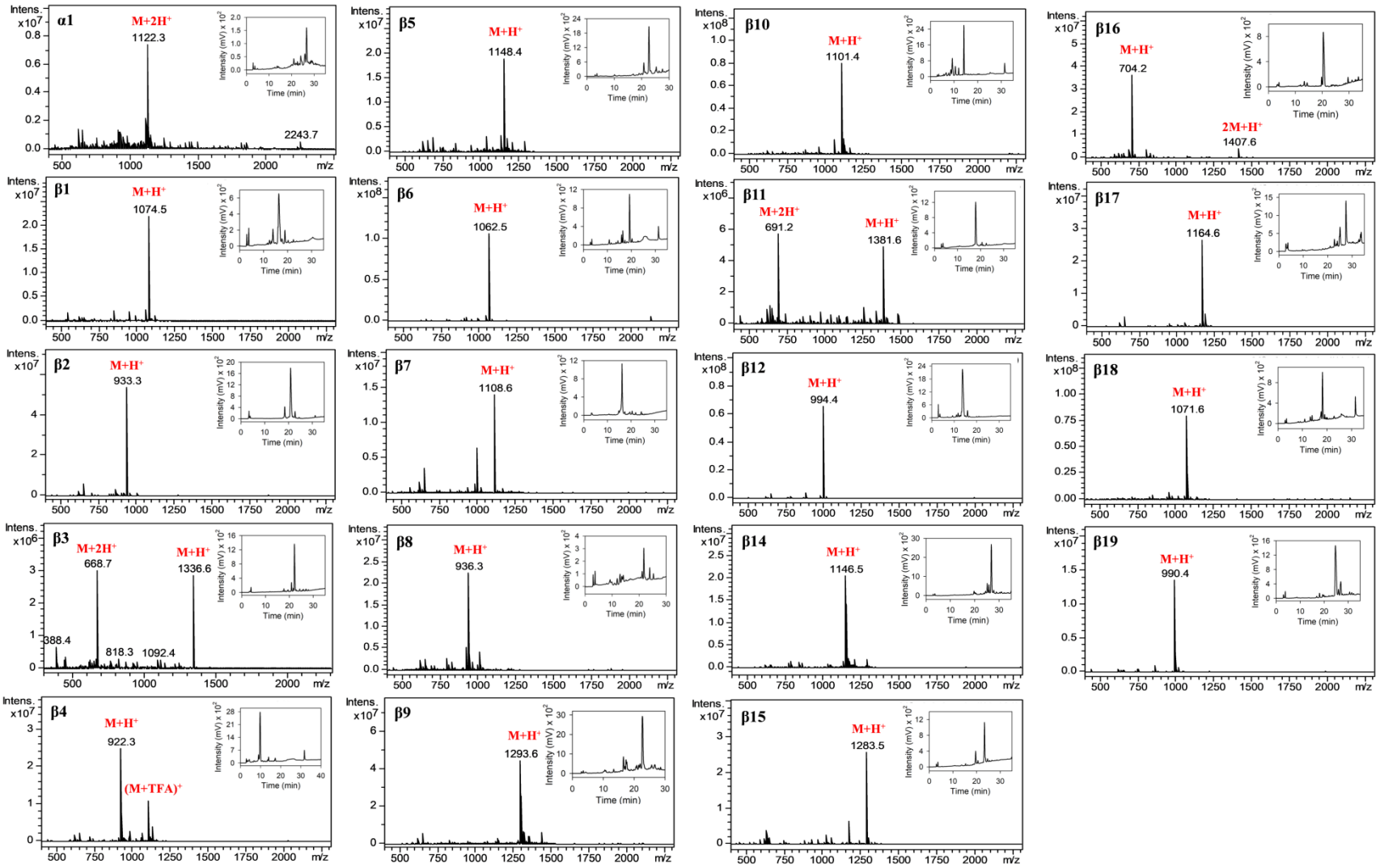

Figure S3. Mass spectra and analytical RP-HPLC profiles of hV3 peptides. Each graph shows the ESI-MS spectrum highlighting the H^+ and $2H^+$ adducts of the peptide (peptide name provided within each panel). Inset shows the analytical RP-HPLC profile of the crude peptide analyzed using a water-methanol gradient.

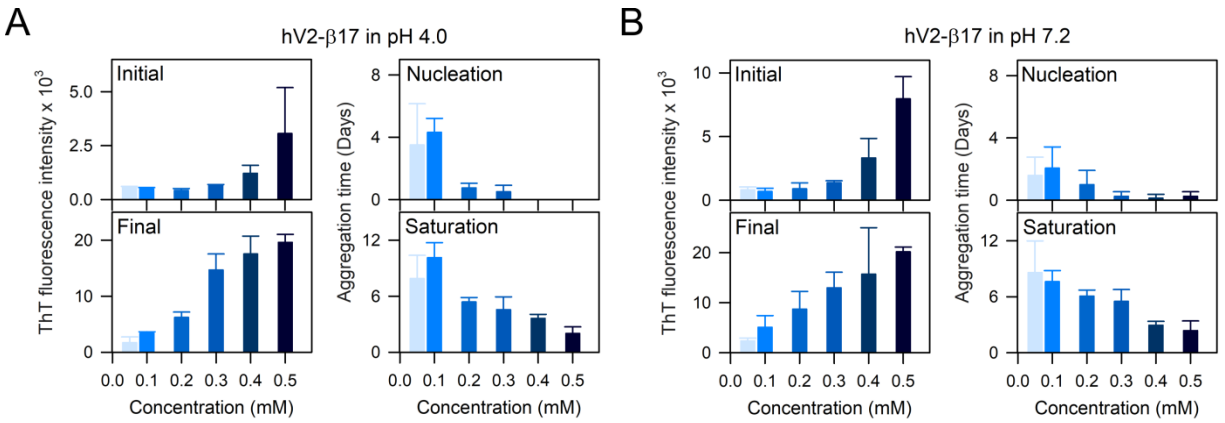

Figure S4 (continued from Figure 1 of the main text). hV2-β17 peptide aggregation properties shown as representative example of peptide-based reverse-mapping approach to chart aggregation hotspots. ThT fluorescence experiments were carried out in pH 4.0 (A) and pH 7.2 (B) at varying hV2-β17 peptide concentrations (0.05 to 0.5 mM; shown as shades of blue). The histograms represent the initial (top) and final (bottom) ThT fluorescence intensity at 485 nm measured at the nucleation and saturation time of peptide aggregation, respectively. As the peptide concentration increases, we observe a concomitant increase in ThT fluorescence and decrease in aggregation time. Similar results are observed in the both buffers (compare (A) and (B)). Error bars represent the standard deviation obtained from three independent experiments.

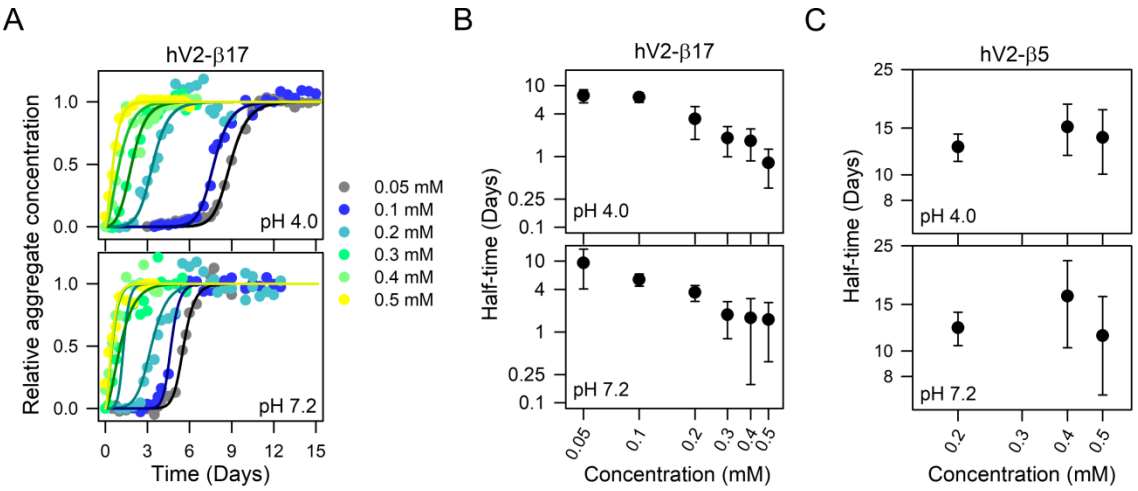

Figure S5 (continued from Figure 1 of the main text). Aggregation half-time calculation from AmyloFit. (A) hV2-β17 shows a concentration dependent increase in aggregation behavior, and serves as a perfect example to understand the molecular mechanism peptide aggregation. Representative aggregation data of hV2-β17 in SCB (upper panel) and SPB (bottom panel) are fitted to the secondary nucleation dominated equation available in AmyloFit.[1] Fits are shown as solid lines. Peptide concentrations were maintained between 0.05 and 0.5 mM (shown on the right). (B).The aggregation half-time of the hV2-β17 decreases from 10 days to 0.5 days with increasing peptide concentration in both SCB and SPB. C).The aggregation half-time of hV2-β5 ranges from 25 to 5 days and does not show a strong concentration dependence. The overall behavior is independent of the buffer conditions (SCB and SPB). All the data were averaged over three independent experiments in (B) and (C).

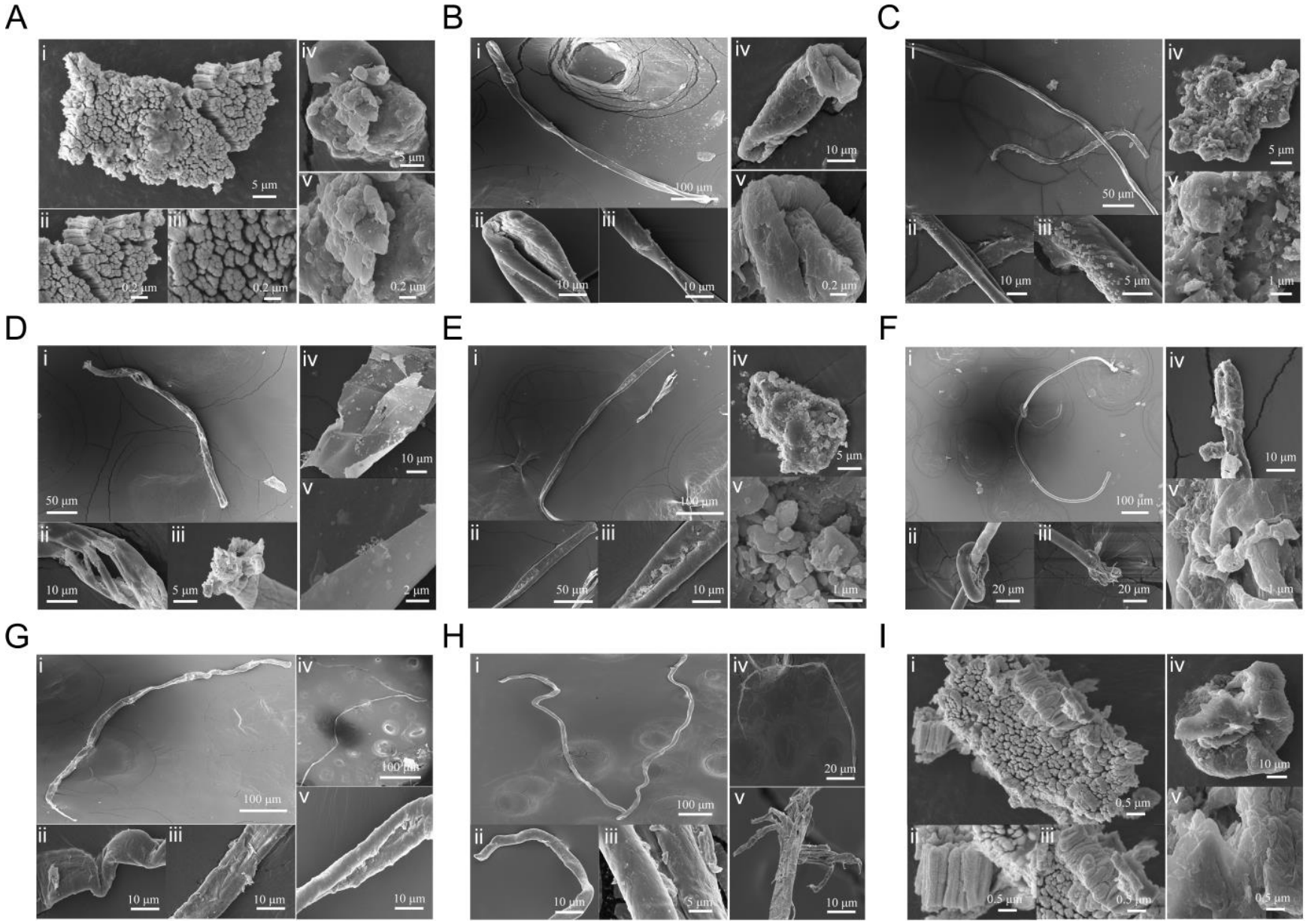
A
i
5 µm
iv
5 µm
v
0.2 µm
ii
0.2 µm
iii
0.2 µm
B
i
100 µm
iv
10 µm
v
0.2 µm
ii
10 µm
iii
10 µm
C
i
50 µm
iv
5 µm
v
1 µm
ii
10 µm
iii
5 µm
D
i
50 µm
iv
10 µm
v
2 µm
ii
10 µm
iii
5 µm
E
i
100 µm
iv
5 µm
v
1 µm
ii
50 µm
iii
10 µm
F
i
100 µm
iv
10 µm
v
1 µm
ii
20 µm
iii
20 µm
G
i
100 µm
iv
100 µm
v
10 µm
ii
10 µm
iii
10 µm
H
i
100 µm
iv
20 µm
v
10 µm
ii
10 µm
iii
5 µm
I
i
0.5 µm
iv
10 µm
v
0.5 µm
ii
0.5 µm
iii
0.5 µm

Figure S6 (continued from Figure 1 of the main text). Representative SEM images of different human VDAC peptides. Aggregated peptide samples (10 μl) were collected from pH 4.0 at the end of a 30-day incubation, and the peptide morphology was visualized by SEM. Representative SEM images for hV1-β5 (A), hV1-β9 (B), hV2-β5 (C), hV2-β8 (D), hV2-β10 (E), hV2-β17 (F), hV3-β6 (G), hV3-β11 (H) and hV3-β17 (I) are presented here. All peptides show the presence of amyloid-like fibrillar aggregates (i – iii) and amorphous aggregates (iv – v). The images for each peptide are presented in different magnifications (low magnification, panels (i) and (iv); high magnification, panels (ii), (iii) and (v)).

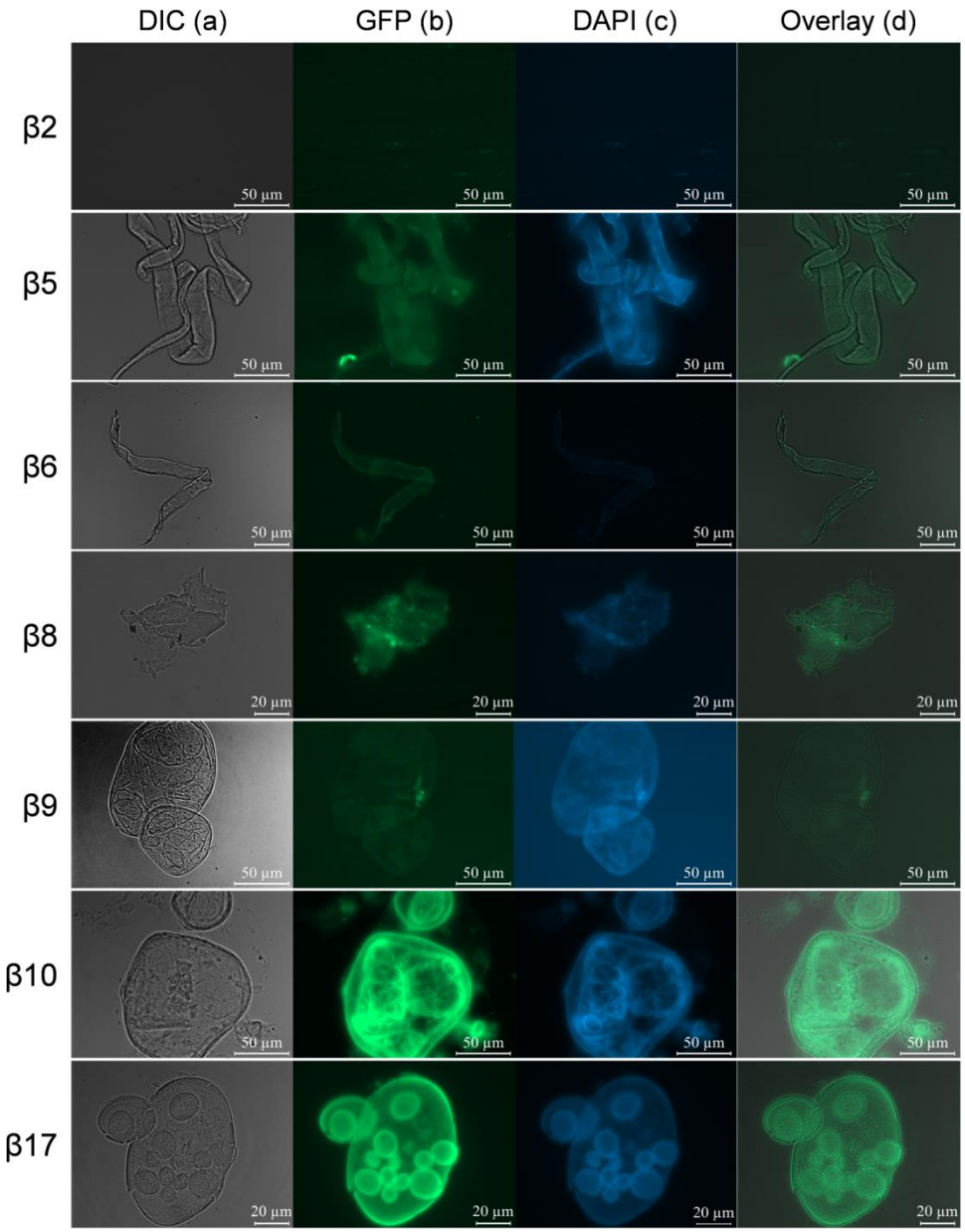

Figure S7 (continued from Figure 1 of the main text). Representative differential interference contrast (DIC) and fluorescence microscopy images of hV2 peptide aggregates. ThT fluorescence was used as a probe to observe the morphology of aggregates structures. The DIC images (a) of representative hV2 peptides (β5–β10 and β17) show the presence of fibrillar or amorphous aggregates, whereas no aggregates were observed in the β2 peptide. The respective images observed in DIC were also visualized using GFP (b) and DAPI (c) filters. The aggregated structures show ThT binding and fluorescence in both detection modes. The overlay of images obtained from DIC and using the GFP filter are shown in panel (d). All the peptides of hV1, hV2, and hV3 that exhibited aggregation showed similar binding to ThT (data not shown).

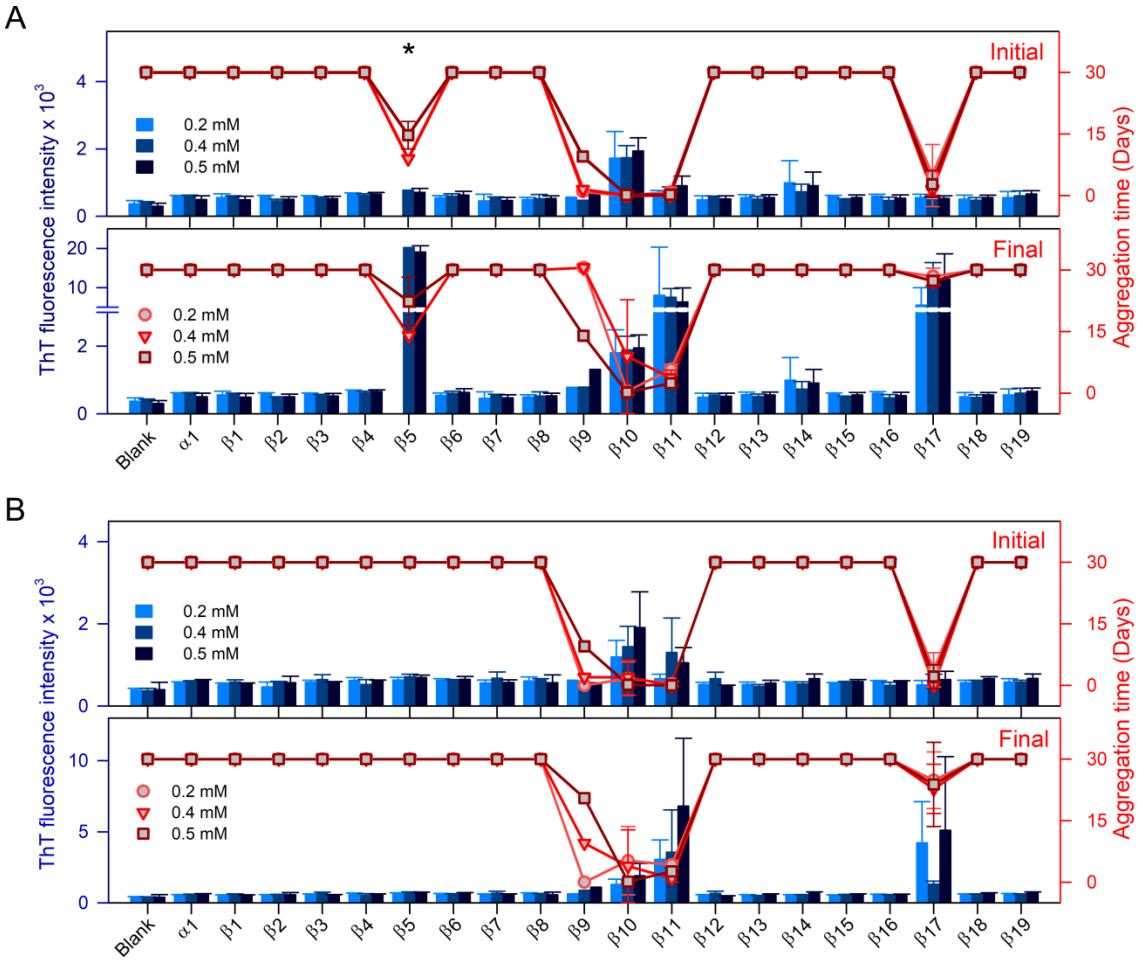

Figure S8 (continued from Figure 2 of the main text). Intrinsic aggregation propensity of hV1 peptides. ThT fluorescence experiments were carried out in pH 4.0 (A) and pH 7.2 (B) at varying peptide concentrations (0.2 mM, 0.4 mM, and 0.5 mM; shown as darker shades of blue or red). The histogram represents the initial (top) and final (bottom) ThT fluorescence intensity at 485 nm (left axis) measured at the nucleation and saturation time of peptide aggregation (scatter plot, right axis). We observed that the strands corresponding to the central region of the protein, namely strands β9–β11, and β17 show significant aggregation propensity and increased ThT binding. We observed inconsistent aggregation in the β5 peptide in all the concentrations (denoted by *) Hence, only the data obtained from instances when aggregation was observed for β5 is plotted here. We observe a concentration–dependent increase in aggregation tendency for all the peptides. Error bars represent the standard deviation obtained from three independent experiments.

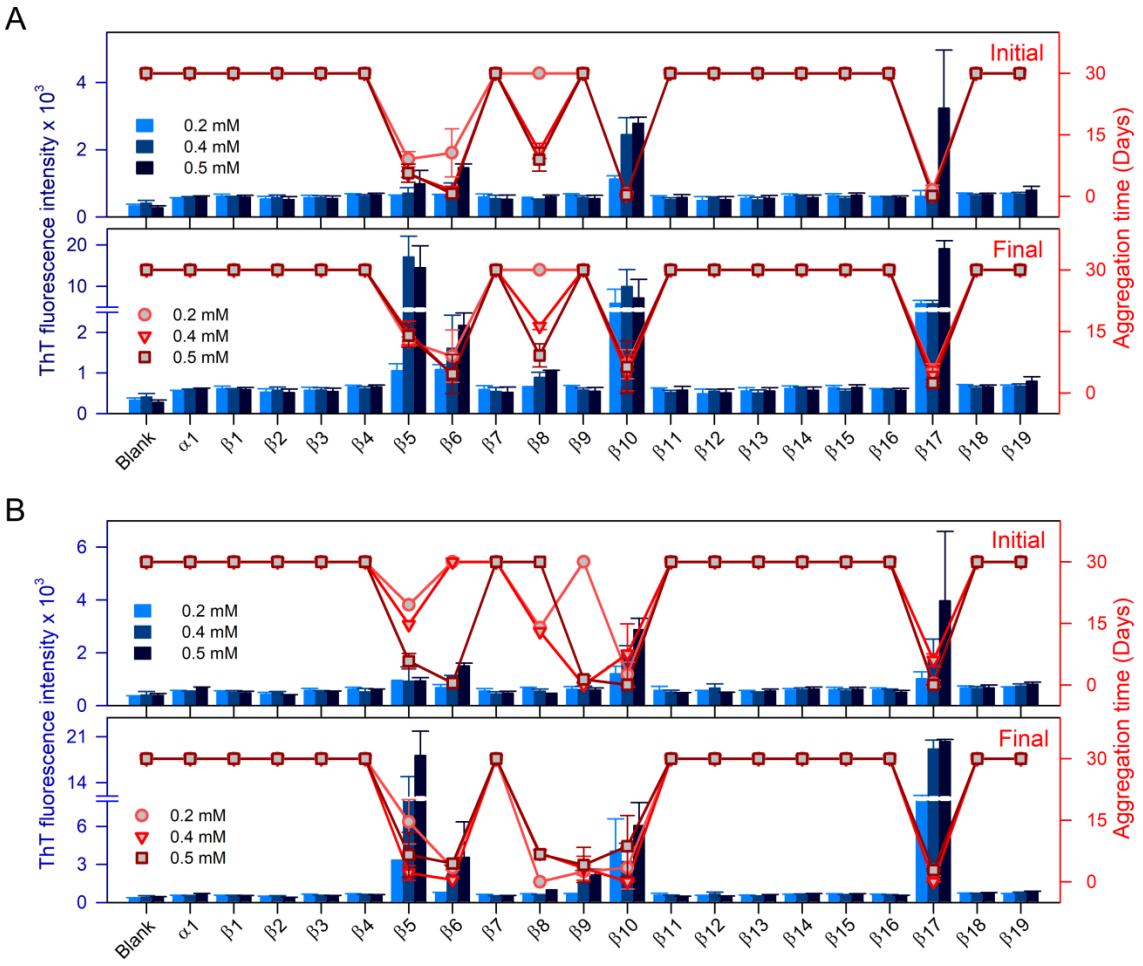

Figure S9 (continued from Figure 2 of the main text). Intrinsic aggregation propensity of hV2 peptides. ThT fluorescence experiments were carried out in pH 4.0 (A) and pH 7.2 (B) at varying peptide concentrations (0.2 mM, 0.4 mM, and 0.5 mM; shown as darker shades of blue or red). The histogram represents the initial (top) and final (bottom) ThT fluorescence intensity at 485 nm (left axis) measured at the nucleation and saturation time of peptide aggregation (scatter plot, right axis). We observed that the strands corresponding to the central region of the protein, namely strands β5–β10, and β17 show significant aggregation propensity and increased ThT binding. Unlike hV1 and hV3, strand β11 of hV2 did not exhibit aggregation, due to subtle variations in its primary sequence (see Figure 3 of the main text). We observe a concentration–dependent increase in aggregation tendency for all the peptides. Error bars represent the standard deviation obtained from three independent experiments.

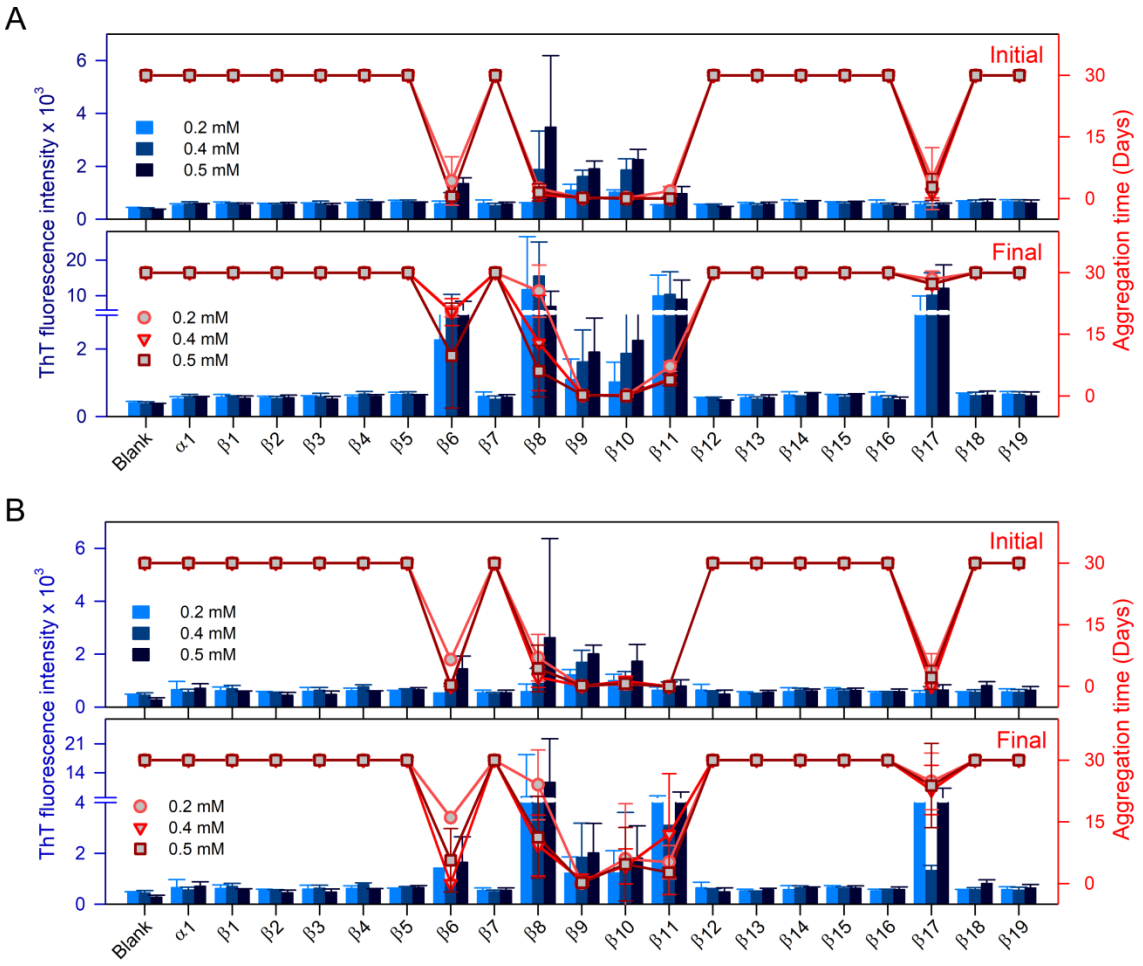

Figure S10 (continued from Figure 2 of the main text). Intrinsic aggregation propensity of hV3 peptides. ThT fluorescence experiments were carried out in pH 4.0 (A) and pH 7.2 (B) at varying peptide concentrations (0.2 mM, 0.4 mM, and 0.5 mM; shown as darker shades of blue or red). The histogram represents the initial (top) and final (bottom) ThT fluorescence intensity at 485 nm (left axis) measured at the nucleation and saturation time of peptide aggregation (scatter plot, right axis). We observed that the strands corresponding to the central region of the protein, namely strands β6–β11, and β17 show significant aggregation propensity and increased ThT binding. We observe a concentration–dependent increase in aggregation tendency for all the peptides. The extent of aggregation varies across the peptides derived from the three proteins, with hV3 showing the highest aggregation tendency of the three isoforms. Error bars represent the standard deviation obtained from three independent experiments.

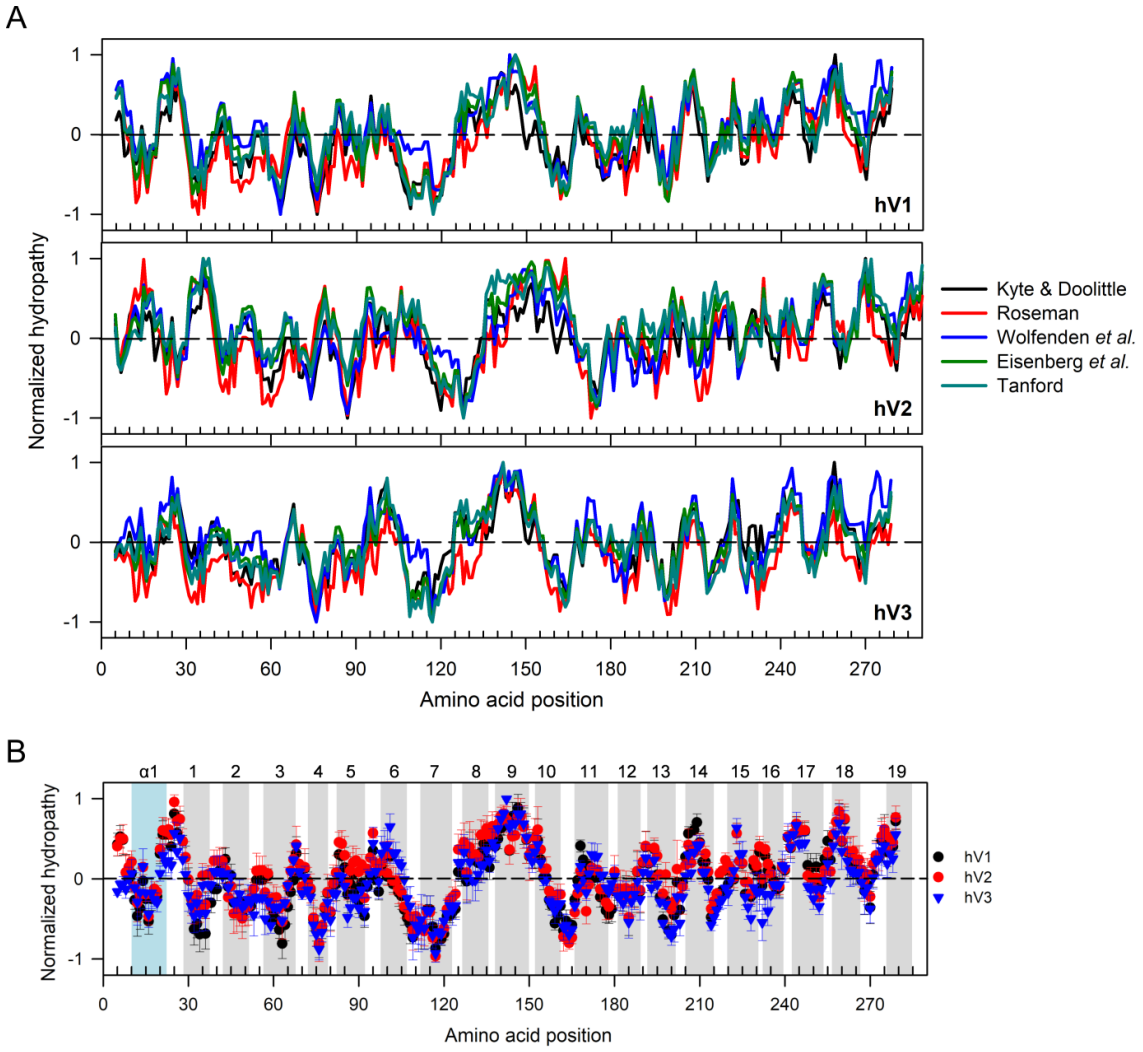

Figure S11. Hydropathy plots for the hVDAC isoforms. Hydropathy plots were calculated using the following well-established scales: Kyte & Doolittle scale (black),[3] Roseman (red),[4] Wolfenden et al., (blue),[5] Eisenberg et al., (green),[6] and Tanford (cyan),[7] scale. The total hydropathy was calculated using a window size of nine residues and the data was normalized between –1 to +1. The region between residues 125 to 155 corresponding to strands β8–β10 in hV1 and hV3 (residues 136 to 166 in hV2) shows a high hydropathy index. Note that hV2 has an additional 11 residues at its N-terminus (termed the N-terminal extension). These residues were not included in the hydropathy index calculation, so as to maintain uniformity across the three human VDAC isoforms. (B) Average hydropathy plots generated from five scales for hV1 (black), hV2 (red) and hV3 (blue), as described in panel A. The numbers above the graph denote the α1 helix and various β-strands (also shown as shaded regions). The average data also shows that the region between residues 125–155 shows a highest hydrophobicity.

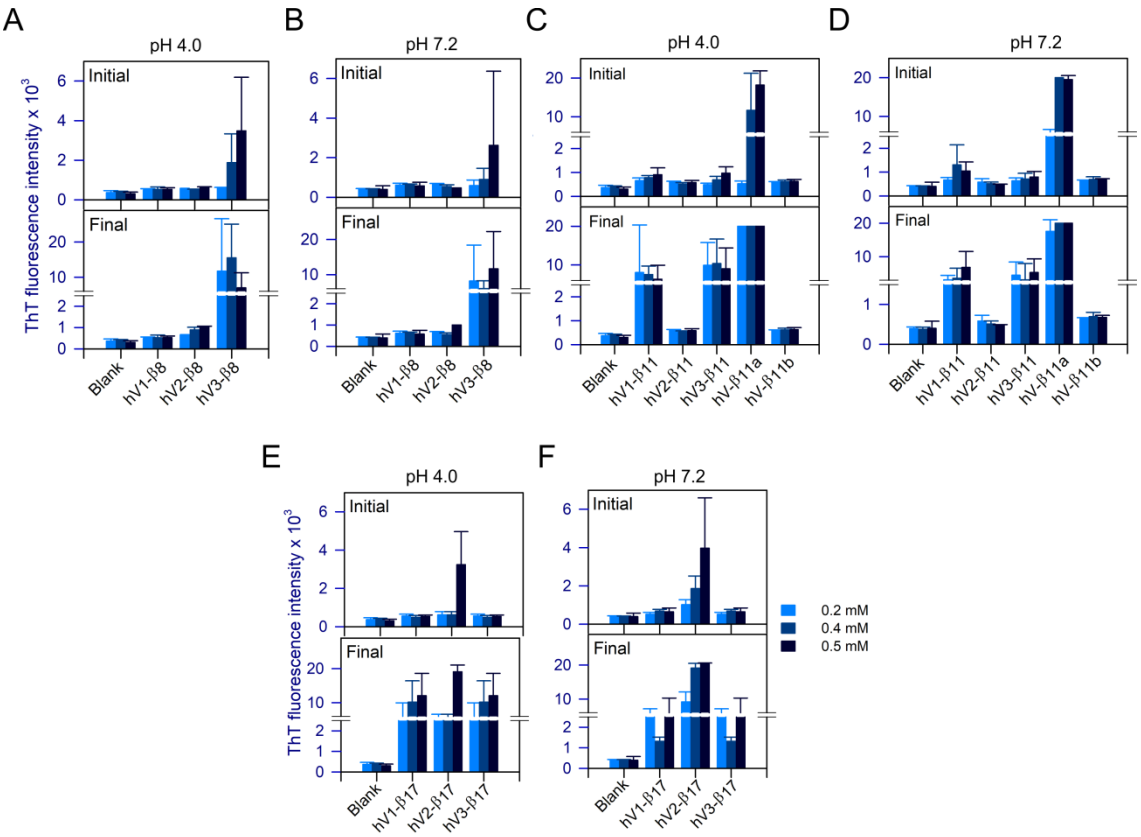

Figure S12 (continued from Figure 3 of the main text). Sequence–driven aggregation propensity of hVDAC peptides. Aggregation propensity of β8, β11 and β17 were compared across the hVDAC proteins. Histograms in each panel represent the initial (top) and final (bottom) ThT fluorescence intensities, denoting nucleation and saturation time of aggregation, respectively, with varying peptide concentration (0.2 mM, 0.4 mM and 0.5 mM; shown as darker shades of blue). Histograms highlight the differences in aggregation tendency of β8, β11 and β17 in pH 4.0 (A, C and E) and pH 7.2 (B, D and F). (A and B) hV3–β8 shows significant aggregation, whereas aggregation of β8 of hV1 and hV2 is negligible. (C and D) Histogram comparing the aggregation tendency of β11 permutants, which is different for all three isoforms. A single residue substitution in hV2-β11 (R166→Q in hV-β11a) shows significant increase in the peptide aggregation. The R174→K substitution (hV-β11b) in hV2-β11 did not show peptide aggregation. (E and F) The parent sequence of β17 across all VDACs has single amino acid difference at position 245 (Leu in hV1/hV3 → Val in hV2). We observe a marginal difference of ThT intensity in pH 4.0, suggesting that all three peptides show comparable aggregation at this pH condition. On the other hand, we observe a 2-fold increase of ThT intensity in pH 7.2 between hV1/hV3 and hV2. The initial ThT intensities are always higher for the peptides that has greater aggregation tendency and suggests that peptide aggregation nucleation is a very early process. These finding suggests that single amino acid is able to dictate the peptide aggregation and it does not depend upon the total hydrophobicity of the peptide.

REFERENCES

(1) Meisl, G.; Kirkegaard, J. B.; Arosio, P.; Michaels, T. C.; Vendruscolo, M.; Dobson, C. M.; Linse, S.; Knowles, T. P. Molecular Mechanisms of Protein Aggregation from Global Fitting of Kinetic Models. *Nat. Protoc.* **2016,** *11*, 252-272.

(2) Ferrone, F. A.; Hofrichter, J.; Eaton, W. A. Kinetics of Sickle Hemoglobin Polymerization. Ii. A Double Nucleation Mechanism. *J. Mol. Biol.* **1985,** *183*, 611-631.

(3) Kyte, J.; Doolittle, R. F. A Simple Method for Displaying the Hydropathic Character of a Protein. *J. Mol. Biol.* **1982,** *157*, 105-132.

(4) Roseman, M. A. Hydrophilicity of Polar Amino Acid Side-Chains Is Markedly Reduced by Flanking Peptide Bonds. *J. Mol. Biol.* **1988,** *200*, 513-522.

(5) Wolfenden, R.; Andersson, L.; Cullis, P. M.; Southgate, C. C. Affinities of Amino Acid Side Chains for Solvent Water. *Biochemistry* **1981,** *20*, 849-855.

(6) Eisenberg, D.; Schwarz, E.; Komaromy, M.; Wall, R. Analysis of Membrane and Surface Protein Sequences with the Hydrophobic Moment Plot. *J. Mol. Biol.* **1984,** *179*, 125-142.

(7) Tanford, C. Contribution of Hydrophobic Interactions to the Stability of the Globular Conformation of Proteins. *J. Am. Chem. Soc.* **1962,** *84*, 4240–4247.